REPORT DOCUMENTATION PAGE

Form Approved
OMB No. 0704-0188

1. REPORT DATE (DD-MM-YYYY)	2. REPORT TYPE	3. DATES COVERED (From - To)
	Technical Papers	

4. TITLE AND SUBTITLE

5a. CONTRACT NUMBER

5b. GRANT NUMBER

5c. PROGRAM ELEMENT NUMBER

6. AUTHOR(S)

5d. PROJECT NUMBER

5e. TASK NUMBER

5f. WORK UNIT NUMBER

7. PERFORMING ORGANIZATION NAME(S) AND ADDRESS(ES)

Air Force Research Laboratory (AFMC)
AFRL/PRS
5 Pollux Drive
Edwards AFB CA 93524-7048

8. PERFORMING ORGANIZATION REPORT

9. SPONSORING / MONITORING AGENCY NAME(S) AND ADDRESS(ES)

Air Force Research Laboratory (AFMC)
AFRL/PRS
5 Pollux Drive
Edwards AFB CA 93524-7048

10. SPONSOR/MONITOR'S ACRONYM(S)

11. SPONSOR/MONITOR'S NUMBER(S)

12. DISTRIBUTION / AVAILABILITY STATEMENT

Approved for public release; distribution unlimited.

13. SUPPLEMENTARY NOTES

14. ABSTRACT

20020827 083

15. SUBJECT TERMS

16. SECURITY CLASSIFICATION OF:			17. LIMITATION OF ABSTRACT	18. NUMBER OF PAGES	19a. NAME OF RESPONSIBLE PERSON
a. REPORT	b. ABSTRACT	c. THIS PAGE			Leilani Richardson
Unclassified	Unclassified	Unclassified	A		19b. TELEPHONE NUMBER (include area code) (661) 275-5015

Standard Form 298 (Rev. 8-98)
Prescribed by ANSI Std. 239.18

41 items enclosed

20050057

MEMORANDUM FOR PRS (Contractor Publication)

FROM: PROI (TI) (STINFO) 06 April 2000

SUBJECT: Authorization for Release of Technical Information, Control Number: **AFRL-PR-ED-TP-2000-062**
Eidelman, S., et al. (SAIC), "Aerothermodynamics of Pulsed Detonation Engines"

AIAA Joint Propulsion Committee (Huntsville, AL, 16-19 July 00) **(Statement A)**
(Deadline unknown)

1. This request has been reviewed by the Foreign Disclosure Office for: a.) appropriateness of distribution statement, b.) military/national critical technology, c.) export controls or distribution restrictions, d.) appropriateness for release to a foreign nation, and e.) technical sensitivity and/or economic sensitivity.
Comments: ______________________________

Signature ______________________ Date ______________

2. This request has been reviewed by the Public Affairs Office for: a.) appropriateness for public release and/or b) possible higher headquarters review
Comments: ______________________________

Signature ______________________ Date ______________

3. This request has been reviewed by the STINFO for: a.) changes if approved as amended, b.) appropriateness of distribution statement, c.) military/national critical technology, d.) economic sensitivity, e.) parallel review completed if required, and f.) format and completion of meeting clearance form if required
Comments: ______________________________

Signature ______________________ Date ______________

4. This request has been reviewed by PRS for: a.) technical accuracy, b.) appropriateness for audience, c.) appropriateness of distribution statement, d.) technical sensitivity and economic sensitivity, e.) military/ national critical technology, and f.) data rights and patentability
Comments: ______________________________

APPROVED/APPROVED AS AMENDED/DISAPPROVED

____
PHILIP A. KESSEL Date
Technical Advisor
Propulsion Science and Advanced Concepts Division

Presented at 36th JANNAF Meeting, Cocoa Beach, FL, 1999

Aerothermodynamics of Pulsed Detonation Engines

Shmuel Eidelman*, Dmitri Sharov*, and David Book+
***SAIC McLean VA 22102 / +Enigmatics Inc., Wash. DC**

ABSTRACT

With no moving parts in the power production section and a thermodynamically efficient cycle, the Pulsed Detonation Engine (PDE) offers a low-cost alternative to turbojet and liquid-propellant rocket engines. Both air-breathing and pure rocket modes of engine operation offer substantial system, materials, and cycle advantages that will allow us to bypass the scalability, operational range, efficiency, and cost limitations of existing engines. We introduced the modern PDE concept in 1986[1] and experimentally demonstrated its operation in 1986[1], 1994[2], and 1998[3]. The concept was subsequently treated extensively in a number of analytical and experimental studies.[2-10]

This paper examines the thermal balance of the PDE as a function of engine length, cycle frequency, external flow Mach number and other parameters. The results indicate that PDEs will have thermal characteristics that are drastically different from conventional engines. The results of the study have important implication for PDE design and analysis.

Introduction

Thermal management is a subject of active discussion in PDE research. One point of view is that PDEs will allow the use of high-energy-density fuels without a need for active cooling or high-cost materials for thermal protection, since the combustion chamber walls are intermittently exposed to hot detonation products and the cold fuel/air mixture, with the cold mixture resident longer in the detonation chamber and therefore playing a bigger role in the PDE thermal balance. Another point of view is that the detonation chamber will overheat as a result of very intense heat exchange with the unsteady flow of detonation products, which for hydrogen/oxygen detonation can reach temperatures in excess of 3500 K. It is known that some groups developing PDEs have a problem keeping the engine walls cool.

Because of the high temperature of the detonation products and high heat transfer rates from the nonsteady flow of hot gases to the detonation chamber walls, detonation chamber cooling is a major design consideration. Analysis of the heat transfer is complicated by the fact that during the purging and refill process the detonation chamber will be filled with cold gases and the heat flux will reverse direction from the hot wall to the gas. In the nonsteady processes of fill, detonation, expansion following detonation, and purge of detonation products, depending on engine design, different parts of the engine will be exposed to different intermittent flow regimes. The problem of heat exchange is compounded by the possible problem of fuel pre-ignition that can occur when the fuel/oxidizer mixture is injected into a very hot detonation chamber. This can result in combustion of the injected mixture instead of detonation and in some cases can convert the chamber into a flame holder that will make subsequent detonations impossible, causing complete loss of thrust.

In this paper we consider the basic dynamics of the PDE heat exchange for a simple engine configuration.

Problem Description

We assume that the PDE device has the simplified configuration shown in Figure 1. The detonation engine consists of a steel tube with 6-cm diameter and 2-mm thickness (in our analysis we will consider various tube lengths). The air is injected through the forward-facing inlets and mixes with fuel injected at the thrust wall. We assume that mixing is very efficient and that for the purposes of our analysis the gaseous fuel/air

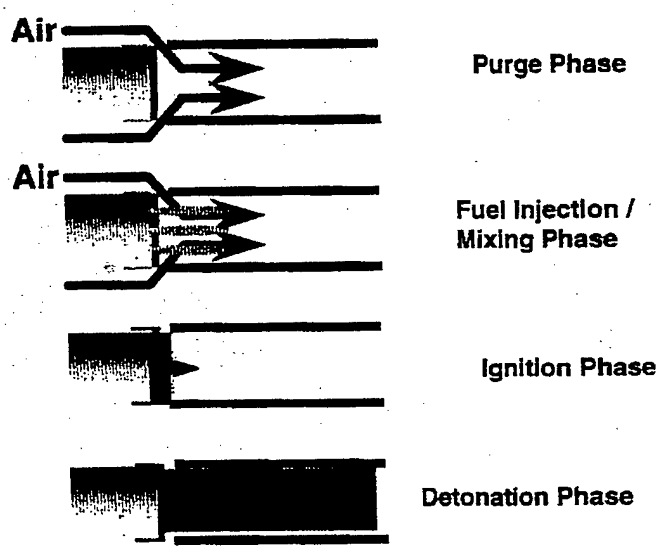

Figure 1. An illustration of the basic phases of an airbreathing PDE cycle.

mixture fills the detonation chamber uniformly. Detonation is initiated at the thrust wall by a thin layer of high-pressure gas and propagates through the mixture. This is only a general description of the problem. Below in our description of the numerical simulations we will give more details about detonation of the injected mixture and the detonation wave parameters.

The fuel/air mixture has the temperature of the ambient air and fills the detonation chamber gradually, with a filling rate such that detonation is initiated at the instant when the mixture reaches the open end of the detonation chamber. The cycle period consist of the time needed to fill the detonation chamber at a certain rate and the time it takes for the detonation wave to propagate through the mixture and for the detonation products to fully expand, producing thrust. Thus, for example, if the detonation engine is 1 m long and operates at 100 Hz and we know that the detonation and expansion processes take 4 msec we assume that the fuel/air mixture is injected into the chamber at 167 m/sec to allow complete filling of the detonation chamber in 6 msec.

Numerical Simulations

It is feasible to find the heat flux to the wall during the process of injection, mixing, detonation, and detonation product expansion through numerical solution of the time-dependent Navier-Stokes equations describing viscous, reactive, and turbulent flow regimes. Calculated heat fluxes to the wall can be used as boundary conditions for the heat transfer problem through the solid walls of the PDE. Such a computation can be very time and resource-consuming and at the end its results cannot be fully trusted and would need experimental validation because of the ambiguities related to selection of the turbulence model and spatial resolution requirements needed to resolve boundary and mixing layers. Although direct Navier-Stokes simulations of the heat flux in PDE devices should be pursued in the future, in this study we adopted a simpler approach that allows rapid evaluation of the PDE wall temperature using PC-based simulations.

In our study we use solutions of the Euler equations to simulate detonation and expansion processes using a methodology that we previously developed for simulations of these processes in PDEs (see References 2-10 for details). We assumed that the PDE has the simple cylindrical geometry shown in Figure 1, where the tube diameter is 6 cm. We also assumed that the inlets are closed during the detonation and expansion processes. The detonable mixture of stoichiometric hydrogen/air at 1 atm and 300 K is initiated by a 2 mm vertical layer at a pressure of 30 atm located at the thrust wall. The numerical simulation gives us the history of the gas-dynamic parameters such as temperature, velocity, and density on both internal and external surfaces of the engine.

In Figures 2, 3, and 4 we show the results of simulating detonation and expansion processes in the form of pressure, velocity, and temperature time histories for a 17 cm-long PDE configuration. We assumed that the engine operates at 100 Hz. The injection of the cold mixture begins 1 msec after initiation. As we see from the pressure plots, 1 msec after detonation the pressure inside the chamber has the ambient value. It is interesting to observe that during the detonation and expansion processes all points along the detonation chamber experience the same pressure and velocity conditions (except during a short period when the detonation wave propagates and transition to the C-J condition takes place). However, the temperature regimes experienced by the locations along the wall are a very strong function of location as is evident from Figure 4. The point 2 cm from the thrust wall will be at a high temperature of ~2000 K only 2 msec and at 300 K for 8 msec. At the same time, the point at 10 cm from the wall will be exposed 7 msec to ~2000 K and 3 msec to 300 K. The points near the end of the detonation tube will have a lower temperature at the end of the expansion cycle due to suction of the ambient air after the initial overexpansion of the detonation products.

We assume that the PDE device is flying with a given flight Mach number at sea-level conditions, where the external flow is cooling the detonation chamber wall. The parameters obtained as a result of simulation of the detonation and expansion processes and the parameters of the external flow over the PDE are used as boundary conditions for the heat transfer problem, which is solved for every point along the engine wall.

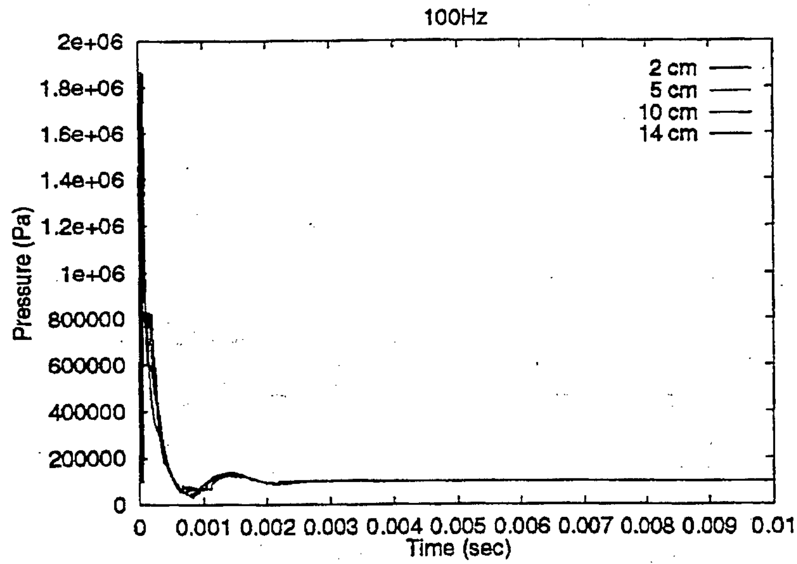

Figure 2. Pressure time history at different locations of the PDE detonation chamber as function of cycle time for a 17-cm-long engine operating at 100 Hz.

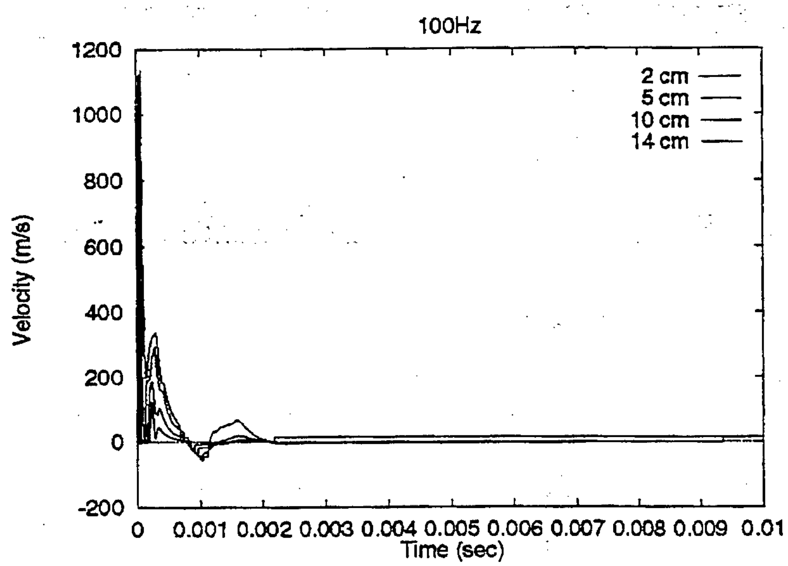

Figure 3. Velocity time history at different locations of the PDE detonation chamber as function of cycle time for a 17-cm-long engine operating at 100 Hz.

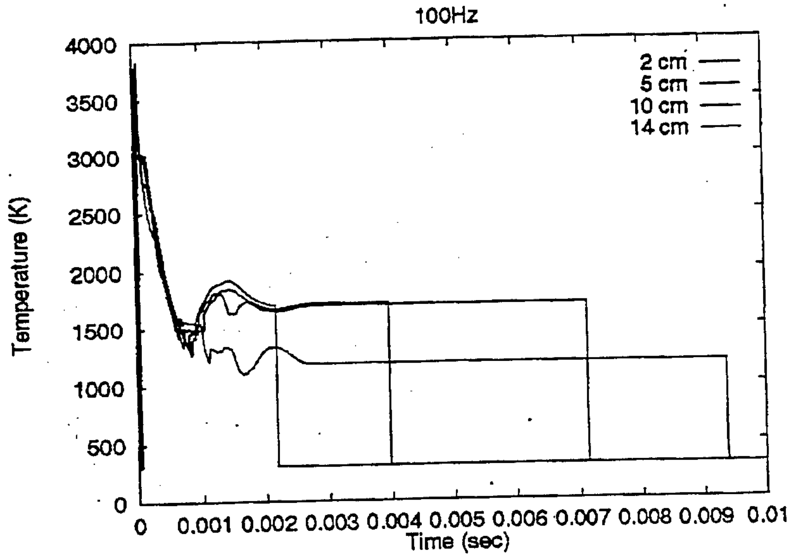

Figure 4. Temperature time history at different locations of the PDE detonation chamber as function of cycle time for a 17-cm-long engine operating at 100 Hz.

The heat transfer problem is described by the heat transfer equation in cylindrical coordinates:

$$\frac{\partial T}{\partial t} = \kappa\left(\frac{\partial^2 T}{\partial r^2} + \frac{1}{r}\frac{\partial T}{\partial r}\right)$$

The boundary condition at $r=R_1$ is

$$-\frac{\partial T}{\partial r} = \frac{h}{k_w}\left(T_{R_1} - T_g\right)$$

The boundary condition at $r=R_2$ is

$$\frac{\partial T}{\partial r} = \frac{h}{k_w}\left(T_{R_2} - T_g\right)$$

$$h = \frac{Nu \cdot k}{l}, \qquad \kappa = \frac{k_w}{C_{pw}\rho_w},$$

where h is the heat transfer coefficient for the gas; k_w is the thermal conductivity for the wall; k is the thermal conductivity for the gas; and l is the length scale. In our calculations we used κ=12.5x10^{-6} m^2/s (steel), k_w =45.4 W/(m K) and

$k = \frac{\gamma R}{\gamma - 1}\mu \Pr$, where Pr =0.72 and γ=1.4

The viscosity μ is computed from the Sutherland law.

The Nusselt number on the external surface of the engine is calculated using the formula for turbulent flow over a flat plate, which according to Reference 11 is also applicable for external flow over a cylinder:

$$Nu = 0.03\,\mathrm{Re}^{0.8}\,\mathrm{Pr}^{0.43}$$

The scaled length used for calculating the Reynolds number is equal to the distance from the thrust wall.

The Nusselt number on the internal surface of the engine is calculated using the turbulent flow in the tube approximation:

$$Nu = 0.021\,\mathrm{Re}^{0.8}\,\mathrm{Pr}^{0.43}$$

Here the length scale used for the Reynolds number calculation is equal to the internal diameter of the tube.

In all calculations we assumed that the next injection is started 1ms after the ignition of the previous portion of the detonable mixture. As explained above, the speed of the fuel/air injections for different cases was adjusted to allow complete filling of the detonation chamber volume for a given cycle period. In Table 1 we list the injection speeds that were used in different simulations.

Table I. Injection speed (m/sec) for different engine length and operation frequency.

Engine length	**Engine operation frequency**			
	50Hz	***100Hz***	***200Hz***	***400Hz***
17cm	7.5 m/s	16.7 m/s	37.5 m/s	100.0 m/s
34cm	15.8 m/s	33.3 m/s	75.0 m/s	–
64cm	31.5 m/s	66.6 m/s	150.0 m/s	–

Results

Our methodology allowed us to simulate the PDE wall temperature as a function of time, engine length, external flow Mach number, and engine operation frequency. To examine the effect of only the four parameters listed above we performed all the simulations for a hydrogen/air detonation in a 6-cm-diameter engine; however, this is not a limitation of our methodology, which can be used to calculate thermal balance for complex geometries and other detonable mixtures.

In Figure 5 we show engine wall temperature as a function of time and distance from the thrust wall for a 34-cm-long engine operating at 100 Hz in an M=0.3 external flow. We see in this picture that the wall temperature will reach steady-state values only after 60 sec of engine operation (or 6000 cycles). Note that we assumed a wall thickness of 2mm; for thicker walls or lower heat conductivity the time required to stabilize the temperature can be even longer. This property implies that the heat losses of the PDE cycle are low, which is another indication of cycle efficiency. The relatively slow heating of the wall can be exploited in engine design, particularly for engines with short operating times. By choosing materials with a low heat transfer coefficient one can operate in transient mode for minutes.

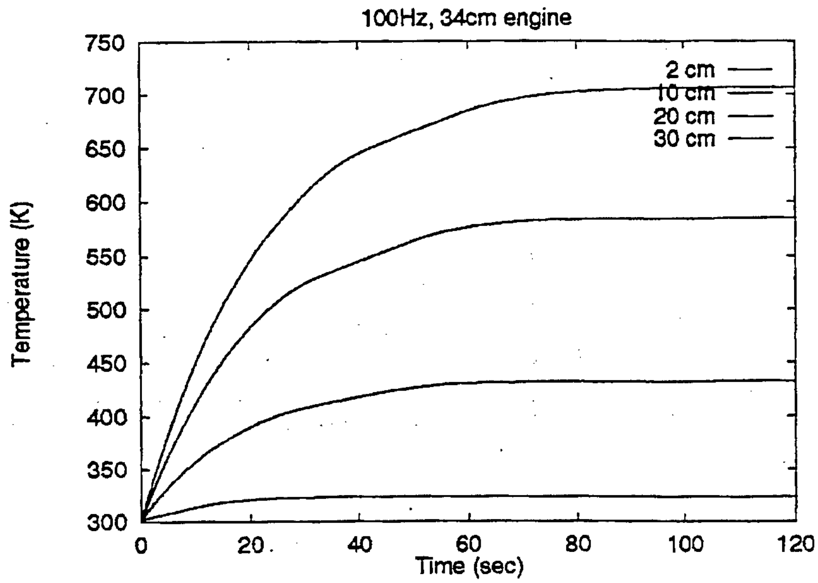

Figure 5. Engine wall temperature as a function of time and distance from the thrust wall for a 34 cm long engine operating at 100 Hz in M=0.3 external flow.

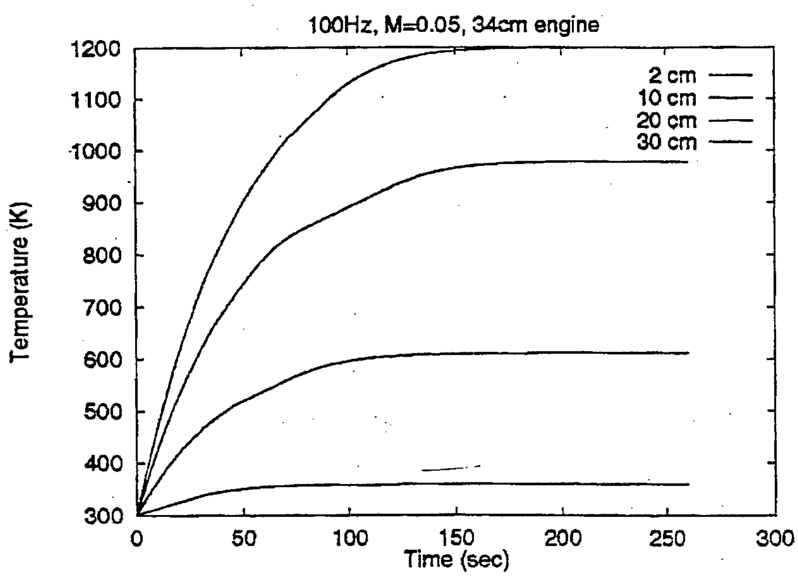

Figure 6. Engine wall temperature as a function of time and distance from the thrust wall for a 34 cm long engine operating at 100 Hz in M=0.05 external flow.

Another property that is clearly identifiable from Figure 5 is that the wall temperature is a strong function of the axial distance from the thrust wall. The engine wall temperature 2 cm from the thrust wall is 320 K, while that at the aft end the wall reaches 710 K. This can be explained by the different time of exposure to hot and cold gas at these locations. The section of the engine 2 cm from the wall be exposed most of the time to the cold flow of injected mixture, while the point at the aft end will be exposed to the cold mixture for a very short time.

In Figure 6 we show wall temperatures for the same engine as in Figure 5, operating in a Mach = 0.05 external flow. Here we see that the engine wall temperature can reach 1200 K. However, it is interesting to note that the wall heats up significantly more slowly than in previous case. It takes twice as long to reach maximum temperature in the *M*=0.05 external flow as in the *M* = 0.3 external flow.

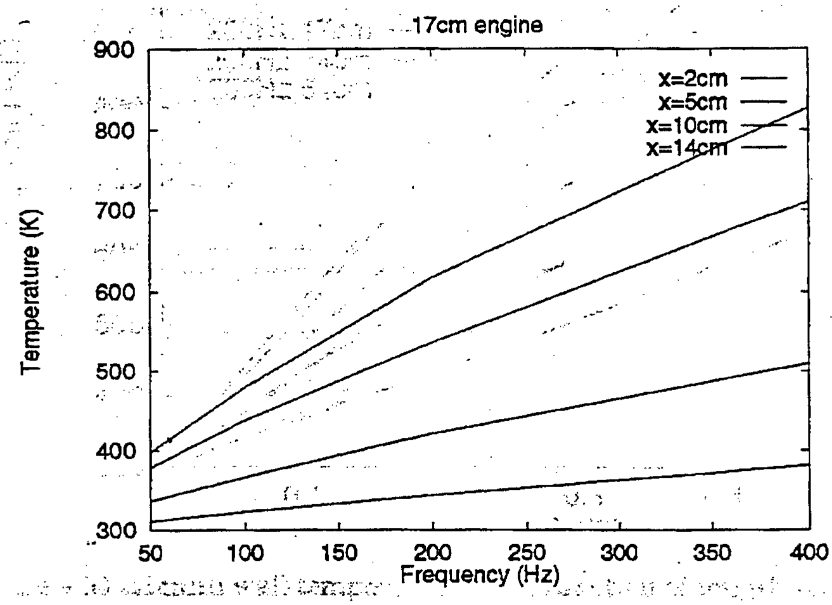

Figure 7. Engine wall temperature as a function of operating frequency for a 17 cm engine operating at Mach = 0.3 external flow conditions.

In Figure 7 we examine the maximum wall temperature at different locations as a function of engine operating frequency for a 17-cm-long engine operating in *M*=0.3 external flow conditions. This figure illustrates that the wall temperature is a linear function of frequency. The wall temperature increase is almost exactly proportional to frequency increase. Thus, an eight-fold increase in frequency (and power density) from 50 Hz to 400 Hz leads to about an eight-fold increase in the wall temperature difference and ambient temperature. This is true for all locations, but the wall section near the aft end where the effects of overexpansion and suction of the ambient air make this relation between the temperature and frequency more complicated.

In Figure 8 we present a summary of our simulation results for 17-cm, 34-cm, and 64-cm-long PDEs operating at 50 to 200 Hz. All simulations where conducted at Mach = 0.3 flight conditions. This figure shows that longer engines will heat up substantially even when operated at a relatively low 100 Hz frequency. The maximum temperature reached in the aft section is a function of the thrust generated by the engine. For example, a 34-cm engine operating at 200 Hz will produce about the same thrust as a 64-cm engine operating at 100 Hz, and they will have about same maximum temperature at the aft section. The same is true for a 17-cm device operating at 200 Hz and a 64-cm device operating at 50 Hz.

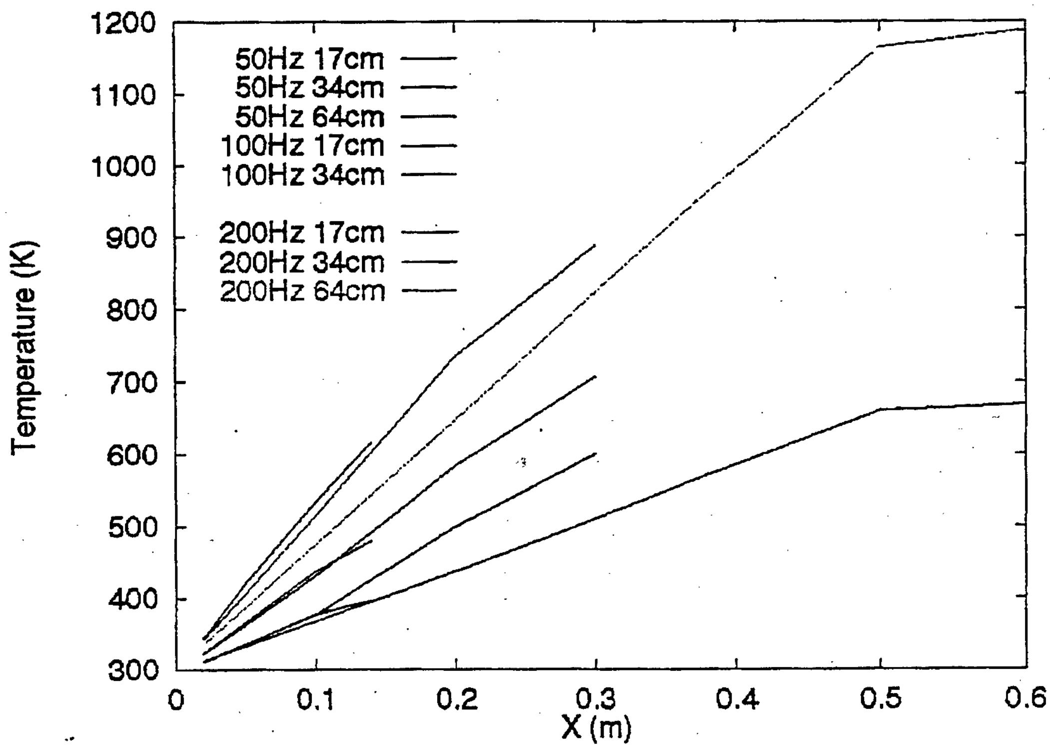

Figure 8 Maximum wall temperatures as a function of length for PDEs operating at different frequencies and at Mach=0.3 external flow conditions.

Conclusions

We have developed a methodology that allows numerical simulation of the PDE wall temperature and heat losses. Using this methodology we examined the main trends of detonation chamber wall temperature dependence on engine length, frequency, external Mach number, and time. Although demonstrated for simple cylindrical configuration, this methodology is general and it can be used for evaluation of the wall temperatures of complex 3-D PDE designs. As a result of our study we can draw the following conclusions:

- Due to the intermittent exposure to cold and hot gas the PDE wall will heat up relatively slowly reaching maximum values for the simulated configuration in 1 to 2 minutes after engine start.

- The PDE will reach its final temperature more quickly for higher subsonic flight Mach numbers;
- For the chosen cylindrical configuration, the wall temperature will increase as a linear function of distance from the thrust wall, and the sections closer to aft end will be the hottest;
- Longer engines will reach higher maximum wall temperatures for the same engine operating frequency;
- Wall temperature increases linearly as the engine frequency increases;
- For the chosen PDE configurations the maximum engine temperature is a function of engine thrust regardless of the frequency and length combination that allows us to obtain the thrust value.

The new simulation methodology can be used to design PDE configurations that will not need forced cooling, thus significantly simplifying engine design.

References

1. Helman, D., Shreeve, R. P., and Eidelman, S., "Detonation Pulse Engine," AIAA-86-1683, 2nd Joint Propulsion Conference, Huntsville, 1986.

2. Eidelman, S., Grossmann, W., Gunners, N.-E., and Lottati, I., "Progress in Pulsed Detonation Engine Development," AIAA-94-2721, June 1994, Indianapolis, IN.

3. Eidelman S., Yang, X., "Analysis of Pulse Detonation Engine Efficiency," AIAA 98-3877, 34th AIAA/ASME Joint Propulsion Conference, Cleveland, OH, 1998.

4. Eidelman, S., Grossmann, W., and Lottati, I., "Propulsion Applications of the Pulsed Detonation Engine Concept," SAIC Report Number 89/1684, 12/ 31, 1989.

5. Eidelman, S. and Grossmann, W., "Computational Analysis of Pulsed Detonation Engines and Applications," AIAA-90-0460, Reno, Nevada, January 8-11, 1990. AIAA Paper 89-2446

6. Eidelman, S., Grossmann, W., and Lottati, I., "Air-Breathing Pulsed Detonation Engine Concept; A Numerical Study," AIAA-90-2420, Orlando, FL, July, 1990.

7. Eidelman, S., et al., "A Review of Propulsion Applications of the Pulsed Detonation Engine Concept," J. Prop. and Pow., V. 7, N6, 1991 (857-865).

8. Eidelman, S., et al, "Pulsed Detonation Engine Experimental and Theoretical Review," AIAA-92-3168, AIAA/ASME 28th Joint Propul. Conf., Nashville, 1992.

9. Eidelman, S., et al., "A Parametric Study of the Air-Breathing Pulsed Detonation Engine," AIAA-92-0392, Reno, Nevada, January 6-9, 1992.

10. Eidelman, S., Yang, X., and Lottati, I., "Pulsed Detonation Engine: Key Issues," AIAA-95-2754, AIAA/ASME 31st Joint Propulsion Conference, San Diego, 1995.

11. Krasnov N., Koshevoy V., Danilov A., "Aerodynamics of rockets", page 557, In Russian, Vishaia Shkola Publishing, 1968.